C. R. Physique 19 (2018) 599–611

Contents lists available at ScienceDirect

Comptes Rendus Physique

www.sciencedirect.com

Physics and arts / Physique et arts

Simulating the composition and structuration of coloring layers in historical painting from non-invasive spectral reflectance measurements

Simuler la composition et la structure de couches picturales historiques à partir de mesures non invasives en spectroscopie de réflexion diffuse

Fabien Pottier [a,*], Morgane Gerardin [b], Anne Michelin [a], Mathieu Hébert [c], Christine Andraud [a]

[a] *Centre de recherche sur la conservation (CRC), MNHN, Sorbonne Universités CNRS, MCC, USR 3224, CP21, 36, rue Geoffroy-Saint-Hilaire, 75005 Paris, France*
[b] *Institut d'optique – Graduate School, 16, rue du Professeur-Benoît-Lauras, 42000 Saint-Étienne, France*
[c] *Univ Lyon, UJM–Saint-Étienne, CNRS, Institut d'optique – Graduate School, Laboratoire Hubert-Curien, UMR 5516, 42023 Saint-Étienne, France*

ARTICLE INFO

Article history:
Available online 17 October 2018

Keywords:
Pictorial layer
Diffuse reflectance spectroscopy
Composition and structuration simulations

Mots-clés :
Couche picturale
Spectroscopie de réflection diffuse
Simulation de composition et de structure

ABSTRACT

Reflectance spectroscopy is a powerful non-invasive technique for determining the material composition of historical polychromies, since the measurement is fast, simple, and contactless. However, reflectance spectra of complex color mixtures can sometimes be hard to interpret from a compositional point of view. In these cases, theoretical optical simulations can provide useful additional data. The main issue is the choice of the optical model that must be adapted to the measurement protocol and the material structure of the coloring layer, this latter being generally unknown. Simple models based on analytical formulas are preferred, as they can be easily inversed to deduce the optical and structural properties of the materials from the measured spectral reflectance of the object. In this paper, we address this issue to investigate the material composition of the colors of the Codex Borbonicus, a 16th-century Mesoamerican manuscript. Two models dedicated to two different types of material structures are presented: the Kubelka–Munk model with Saunderson correction, suitable for one homogenous layer, and the Clapper–Yule model used for continuous colorant layer, suitable when a weakly scattering paint is on top of a diffusing support. The results of the simulation provide new insights into the way the coloring materials were combined in the document, either as mechanical mixture before application or as superimposition.

RÉSUMÉ

La spectroscopie de réflexion diffuse est une technique non invasive très pratique pour l'étude des polychromies historiques, puisque sa mise œuvre est rapide, simple et sans

* Corresponding author.
E-mail address: fabien.pottier@mnhn.fr (F. Pottier).

https://doi.org/10.1016/j.crhy.2018.09.007

contact. Toutefois, les spectres de réflexion de mélanges colorés complexes peuvent parfois être difficiles à interpréter d'un point de vue compositionnel. Dans ces cas, des simulations optiques théoriques peuvent fournir des données supplémentaires pertinentes. La problématique principale concerne le choix du modèle optique, qui doit être adapté au protocole de mesure et à la structure matérielle (généralement inconnue) des couches colorées étudiées. Les modèles simples basés sur des formules analytiques sont préférés, puisqu'ils peuvent facilement être inversés pour déduire les propriétés optiques et la structure des matériaux à partir de leur réflectance spectrale. Dans cet article, cette problématique est abordée pour l'étude de la composition des peintures du Codex Borbonicus, un manuscrit mésoaméricain du XVI^{e} siècle. Deux modèles sont appliqués pour deux types de structure matérielle : le modèle de Kubelka–Munk avec la correction de Saunderson, adapté à une couche colorée homogène, et le modèle de Clapper–Yule pour des couches continues de colorants, adapté à une peinture faiblement diffusante superposée à un support diffusant. Les simulations apportent une nouvelle compréhension quant à la façon dont les matériaux colorants ont été associés dans le document, soit par mélange mécanique avant application, soit par superposition.

1. Introduction

Diffuse reflectance spectroscopy in the visible range is a common analytical technique for the characterization of coloring materials in the cultural heritage domain. Its light weight instrumentation is easy to move in museums or archaeological sites, it only requires an exposure of the studied object to a low-intensity halogen light, and each spectral acquisition only takes a few seconds. Most coloring materials have wide absorption bands in the visible range, and some of them exhibit unique absorption specificities that help their identification. For example, insect derived anthraquinonic red lakes present local absorption maxima at 495, 525, and 560 nm [1]. Hence, when encountering pure compounds in a work of art, the interpretation of the spectra is generally possible and facilitated by comparison with spectral databases [2–7]. However, when pigments are present in mixtures, the resulting spectra are non-linear combinations of the spectral contribution of the different compounds. In these cases, the "spectral signature" of each compound (i.e. the position and the shape of the absorption edge) is altered. As a result, it is almost impossible to characterize the complex material composition unless additional data is found.

Diffuse reflectance spectroscopy can be of interest to investigate the paint composition by comparing the measured spectra with simulations with optical models for plausible coloring material associations. During the study of a polychromatic object, different coloring preparations can be characterized on different colored areas (e.g., blue or yellow). It is plausible that the same "primary" color preparations are combined to create tone variations or other colors (e.g., green) elsewhere on the same object. One can get confirmation of this hypothesis by combining, thanks to an appropriate model, the optical properties of the "primary" colorants deduced from the spectral reflectances measured on the corresponding areas (blue and yellow in the example given above), and see whether the obtained spectral reflectance matches or not the one measured on the area painted with the mixture (green area). From a cultural standpoint, the demonstration of these coloring materials associations is important for the study of ancient objects. In the example, a green can be obtained through the association of the yellow and blue that are used alone in the object, either as a mechanical mixture or as a superimposition. But other materials can also be used in both of these association modalities. Showing that this or that way of obtaining green was preferred in such or such culture could then be interpreted by art historians either in terms of esthetics, taboos, technical choices, access to resources, etc.

Simulating the spectral combination of coloring materials in the visible range is a widespread issue in color science, covering many research and industrial applications (pigment or dye formulation, printing [8], painting [9,10], …). In general, the physical parameters (particle size, refractive index, layer thickness …) of the pure materials are known, or at least measurable, which facilitates the modeling of their absorption and scattering properties. In contrast, during the non-invasive characterization of a historical object, the chemical nature and the physical parameters of the coloring materials are unknown, and it is not possible to sample them for any additional measurement. The only experimental data that are available are the spectral reflectances of the different areas of the object, and hopefully the ones of the underlying substrate in areas when it is uncovered. One should also consider that these historical materials are generally heterogeneous at the macro- and microscales, and organized in a stratified structure. A typical example in easel painting is a slightly absorbing varnish layer on top of an absorbing and scattering colored layer (pigment mixed with a binder), itself on top of a scattering preparation layer (white pigment with a binder). As a result, various case-specific hypotheses must be pronounced regarding the painting composition and structure. Since each of them implies a different way for light of being scattered, absorbed, and finally reflected according to the wavelength, each one is attributed to a specific optical model.

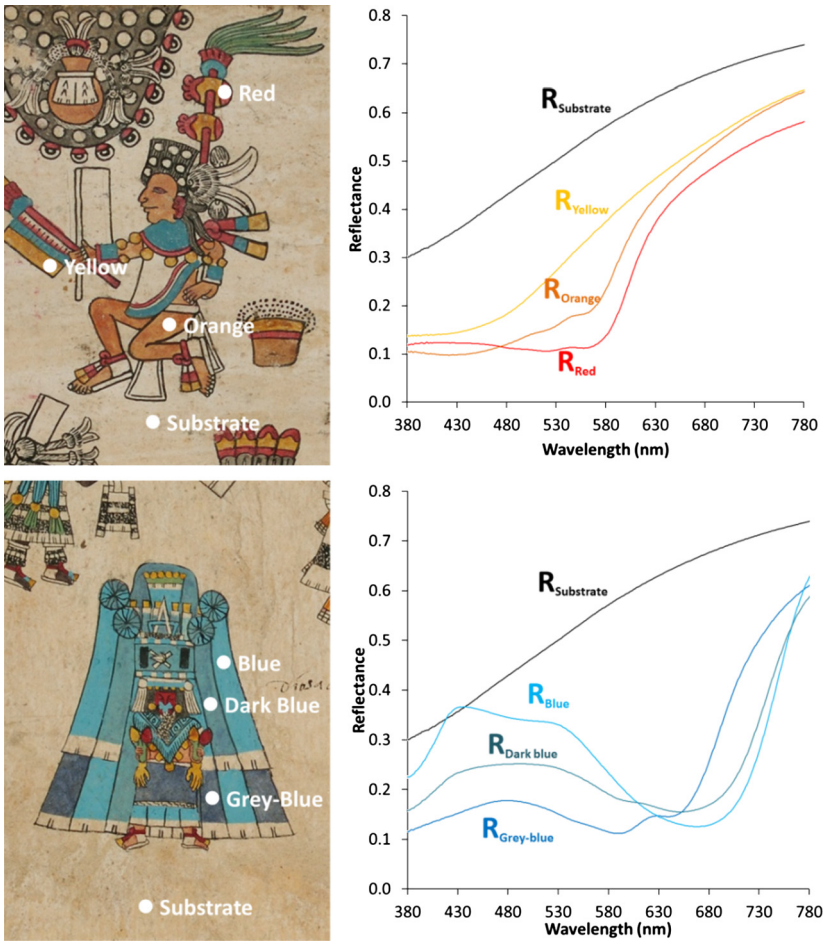

Fig. 1. Pages 8 (top) and 31 (bottom) of the Codex Borbonicus (details, © Bibliothèque de l'Assemblée nationale), along with corresponding representative diffuse spectral reflectances.

In this paper, two modalities of coloring material association (mechanical mixture and superimposition) are considered. Two appropriate spectral reflectance models are presented: the Kubelka–Munk model with Saunderson correction for the mechanical mixture of coloring materials, and the Clapper–Yule model for continuous layers for stacks of coloring layers (see [10–12] for previous works in this field). The hypotheses and simplification that their application requires are presented. As an illustration, the study of the coloring materials associations used in a 16th-century Mesoamerican manuscript is presented.

1.1. Coloring materials in the Codex Borbonicus

The Codex Borbonicus is a 16th-century Aztec manuscript whose coloring materials have been extensively studied with transportable and non-invasive spectroscopies [13–16]. Details of two pages of the manuscript are shown in Fig. 1, in which the colors of the different paints can be observed. Corresponding representative reflectance spectra recorded in these colors are also given.

Experiments. A FieldSpec4 "Hi-Resolution" fiber optic spectrometer (ASD) was used, which covers the visible and shortwave infrared range of the spectrum (350–2500 nm). It is equipped with a halogen light source that is held normal to the sample surface, while the reflected signal is collected at 45° from the normal of the surface. The spectral sampling is of 3 nm in the extended "visible" domain (350–1000 nm). The instrument has been modified in order to prevent any contact between the probe and the document. The distance between the sample and the collecting fiber (1 cm) was kept constant along the measurements. In these conditions, the analyzed surface is about 5 mm in diameter. Spectral reflectances are normalized with a white reference standard measured on a Spectralon® plate that is considered to reflect more than 99% of the light at each wavelength of the spectrum.

The spectral reflectances of the orange and dark-blue paints suggest that red and yellow are combined in the first case, and blue and grey-blue paints are combined in the second case. These hypotheses are based on the spectral reflectance

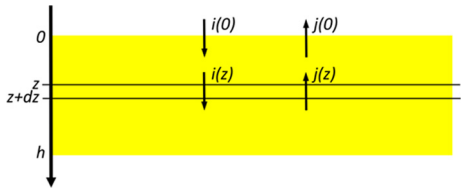

Fig. 2. Upward and downward flux through a sublayer of thickness dz.

shapes: the characteristic absorbance maxima of the red and grey-blue are also found in the orange and dark blue, respectively. Thus, it is probable that the orange color has been produced by mixing the red material with a yellow one, but this is difficult to ascertain as yellow coloring materials do not generally exhibit any spectral characteristic. The first question that we want to answer through our simulations is as follows: once the spectral reflectances of areas painted with the red paint alone, the yellow paint alone, and the orange paint are measured, and their respective optical properties are deduced, do the optical properties of the orange coincide with the one that we can simulate for a mixture of the red and yellow paints?

In the case of the dark-blue color, a visual examination of the color non-homogeneities suggests that, in contrast with the orange color, it has not been obtained by mixing the colors before the application of the paint, but rather by superimposing a layer of grey-blue material on top of a layer of blue material. The second question that we address is the following: can the measured spectral reflectance of the dark-blue paint be matched by a simulated spectral reflectance for the substrate coated by a blue layer then by a grey-blue layer?

2. Theoretical approach

In order to simulate coloring materials associations in the visible range, the main idea is to take into account all interactions between the materials composing the colored object and the visible light to which it is exposed. The Radiative Transfer Equation (RTE) describes the propagation of light in a heterogeneous and disordered medium, consisting of scattering and absorbing particles. The RTE stems from an energy balance and describes the spatial evolution of the light radiance at a given depth, in an elementary layer of the medium, in a given direction. In the case of scattering layers, illuminated by a perfectly diffuse illumination also called Lambertian source, or in the case of very high scattering media, the light intensities inside and outside the media are independent of the direction of propagation, the expression of the RTE is reduced to two equations and leads to the Kubelka–Munk model.

2.1. The Kubelka–Munk model

This model was initially proposed by Kubelka and Munk in 1931 in order to predict the reflectance of paints, by considering them as perfectly isotropic scattering media [17]. In theory, this two-flux model is valid under Lambertian illumination. The Kubelka–Munk model describes, thanks to a simple differential equation system that can be analytically solved, the propagation of two fluxes flowing perpendicularly to the layer in opposite directions (Fig. 2). The variations of these fluxes are due to backscattering and absorption within the layer.

Let's call K the linear absorption coefficient and S the linear scattering coefficient of the medium. By crossing a slice of material with thickness dz, the downward flux $i(z)$ decreases because of absorption and backscattering by an amount proportional to the absorption and the scattering coefficients and to the layer thickness dz. However, it also increases due to the fraction of upward flux $j(z)$ that is backscattered downwards, also proportional to the scattering coefficient and the layer thickness dz. We thus have:

$$\frac{\mathrm{d}i}{\mathrm{d}z} = -(K+S)i(z) + Sj(z) \tag{1}$$

The second equation of the differential system is obtained by analyzing the upward flux $j(z)$ in a similar manner as for $i(z)$, with different signs because of the opposite flux orientations:

$$\frac{\mathrm{d}j}{\mathrm{d}z} = (K+S)j(z) - Si(z) \tag{2}$$

By solving the system composed of Eqs. (1) and (2), we obtain the analytic expressions for the upward and downward fluxes:

$$\begin{cases} i(z) = \dfrac{1}{b}\big[j(0) - ai(0)\big]\sinh(bSz) + i(0)\cosh(bSz) \\ j(z) = \dfrac{1}{b}\big[aj(0) - i(0)\big]\sinh(bSz) + j(0)\cosh(bSz) \end{cases} \tag{3}$$

with $a = \frac{K+S}{S}$ and $b = \sqrt{a^2-1}$.

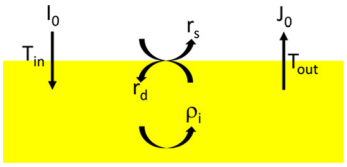

Fig. 3. Saunderson correction at the air interface.

From Eqs. (3), we can derive the expressions for the reflectance ρ_h and the transmittance τ_h of a layer with any thickness h. When the paint layer is illuminated only from the top side, we have therefore: $j(h) = 0$. Eqs. (3) thus yield:

$$\rho_h = \frac{j(0)}{i(0)} = \frac{\sinh(bSh)}{b\cosh(bSh) + a\sinh(bSh)} \tag{4}$$

and

$$\tau_h = \frac{i(h)}{i(0)} = \frac{b}{b\cosh(bSh) + a\sinh(bSh)} \tag{5}$$

2.2. Remission function model

The paint layer is supposed to be homogeneous and infinitely thick, i.e. $h \to \infty$. The limit for the reflectance ρ_h is:

$$\rho_\infty = a - b = \frac{K+S}{S} - \sqrt{\left(\frac{K+S}{S}\right)^2 - 1} \tag{6}$$

We can derive a relation between the ratio K/S, called the *remission function*, and the reflectance of the infinitely thick layer:

$$\frac{K}{S} = \frac{(1-\rho_\infty)^2}{2\rho_\infty} \tag{7}$$

Notice that ρ_∞ is the reflectance of the layer considered without interface between the air and the layer. It depends on the wavelength of light, and so does the remission function.

In the case of a mixture of paints, the remission function follows Duncan's additivity law [9]: since the absorption coefficient (resp. scattering coefficient) of the mixture is the sum of the absorption coefficients (resp. scattering coefficients) of its primary components weighted by their respective proportions c_p, the remission function for the mixture is given by

$$\left(\frac{K}{S}\right)_{\text{Mix}} = \frac{\sum_p c_p K_p}{\sum_p c_p S_p} \tag{8}$$

where K_p and S_p denote the absorption and scattering coefficients of the different components (labeled p) in the mixture, and c_p their respective proportions, which satisfy:

$$\sum_p c_p = 1 \tag{9}$$

2.3. Saunderson correction

The previous equations do not take into consideration the reflections of the light at the paint–air interface, which generally have significant influence on the reflectance of the sample even when the surface is rough [18]. The Saunderson correction permits to take these multiple reflections of light into account [19].

Let $\rho_i(\lambda)$ denote the intrinsic reflectance of the colorant i given by the Kubelka–Munk model without interface with air, and $R_i(\lambda)$ the effective reflectance of the sample, which is the one that we measure. We have [8]:

$$R_i(\lambda) = \frac{J_0}{I_0} = r_s + \frac{T_{\text{in}} T_{\text{out}} \rho_i(\lambda)}{1 - r_{\text{d}} \rho_i(\lambda)} \tag{10}$$

where r_s, T_{in}, T_{out}, and r_{d} (see Fig. 3) denote the reflectances and transmittances of the interface, which depend on its relative refractive index and on the angular distribution of light on its two faces. They can be calculated from the Fresnel formulae as follows, by considering the d:45° measurement geometry that we used. Hereinafter, the Fresnel reflectance and transmittance are denoted by $R_{12}(\theta)$, resp. $T_{12}(\theta) = 1 - R_{12}(\theta)$, when the light comes at angle θ from the medium of index

n_1 (air), and as $R_{21}(\theta)$, resp. $T_{21}(\theta) = 1 - R_{21}(\theta)$, when it comes at angle θ from the medium of index n_2 (paint). We usually assume that, for paints, papers and most polymers, $n = 1.5$. For unpolarized light, the reflectance $R_{12}(\theta)$ is given by:

$$R_{12}(\theta) = \frac{1}{2}\left[\left(\frac{\cos(\theta) - \sqrt{n^2 - \sin^2(\theta)}}{\cos(\theta) + \sqrt{n^2 - \sin^2(\theta)}}\right)^2 + \left(\frac{n\cos(\theta) - \sqrt{n^2 - \sin^2(\theta)}}{n\cos(\theta) + \sqrt{n^2 - \sin^2(\theta)}}\right)^2\right] \tag{11}$$

where $n = n_2/n_1$. $R_{21}(\theta)$ is given by similar formula by replacing n with $1/n$.

Although the paints are observed under diffuse light, a small amount of this light is specularly reflected by paints at the observation angle θ. This fraction is described by the parameter r_s.

The parameter r_d is the reflectance of the interface at the paint side, accounting for the diffuse light coming from the whole hemisphere. It is given by [20], [21]:

$$r_d = \int_0^{\frac{\pi}{2}} R_{21}(\theta)\sin(2\theta)\mathrm{d}\theta \tag{12}$$

The parameter T_{in} corresponds to the transmittance of the air interface for the incident light. Since this latter is assumed to be Lambertian, it accounts for the transmission of light over the hemisphere

$$T_{in} = \int_0^{\frac{\pi}{2}} T_{12}(\theta)\sin(2\theta)\mathrm{d}\theta = 1 - \int_0^{\frac{\pi}{2}} R_{12}(\theta)\sin(2\theta)\mathrm{d}\theta \tag{13}$$

The parameter T_{out} corresponds to the transmittance of the interface for the light exiting the material towards the detector.

$$T_{out} = \frac{1 - R_{12}(\theta = 45°)}{n^2} \tag{14}$$

The term $1/n^2$ comes from the changing of geometrical extent due to the refraction through the interface.

The intrinsic reflectance $\rho_i(\lambda)$ of the material can be deduced from the measured one $R_i(\lambda)$, by inversing Eq. (10):

$$\rho_i(\lambda) = \frac{R_i(\lambda) - r_s}{r_d(R_i(\lambda) - r_s) + T_{in}T_{out}} \tag{15}$$

Remission functions are then to be deduced from the intrinsic reflectance obtained.

2.4. The Clapper–Yule model

While the Kubelka–Munk model presented above assumes that the colored layer is a mixture of paint and paper substrate forming a homogenous scattering medium at the macroscopic scale, we propose here to consider an alternative configuration where the paint, assumed to be weakly scattering, remains on top of the diffusing paper substrate. An optical model adapted to this configuration has been introduced by Williams and Clapper in 1953 in the context of gelatin photographs, where the paper is coated by a purely absorbing and non-scattering gelatin layer [22,23]. The same year, Clapper and Yule presented a similar model for halftone prints, where a discontinuous layer of ink is coated onto a paper substrate [24]. In the case where the ink layer is continuous (full coverage of the support), the Williams–Clapper and Clapper–Yule models are comparable: both consider the multiple reflections of light between the substrate and the coating–air interface through the coating. However, there is a difference between the two models regarding the attenuation by absorption of light within the coloring layer: the Williams–Clapper model considers that oblique rays are more attenuated than perpendicular rays as they follow a longer path within the transparent layer, whereas the Clapper–Yule model assumes that every ray is attenuated in the same way independently of its orientation [25]. The Clapper–Yule model looks more appropriate in the case where the coating is slightly scattering, or partly penetrates into the substrate, which is probably the case in the Codex Borbonicus. In the following, we therefore focus on the Clapper–Yule model applied to continuous layers. We assume that the paint layer is uniform, and that the illumination is perfectly diffuse.

The model consists of the description of the multiple reflections of the light between the paint–air interface and the substrate, through the paint layer. The substrate, considered without its interface with air, has an intrinsic reflectance ρ_s that can be deduced from the measure reflectance R_i according to Equation (20). The paint layer has an intrinsic transmittance t_{paint}, and an intrinsic reflectance zero since it is assumed to be very weakly scattering (Fig. 4).

By analyzing the way light is reflected or transmitted by the different components, one can deduce the following expressions for the upward and downward fluxes:

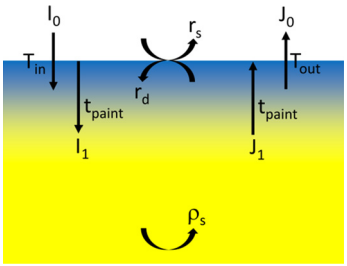

Fig. 4. Multiple reflections considered in the Clapper–Yule model.

$$J_0 = r_s I_0 + T_{out} t_{paint} J_1$$
$$J_1 = \rho_s I_1$$
$$I_1 = T_{in} t_{paint} I_0 + r_d t_{paint}^2 J_1$$

Then, by combining these three equations, we derive the expression of the reflectance of the printed layer:

$$R_i(\lambda) = \frac{J_0(\lambda)}{I_0(\lambda)} = r_s + \frac{T_{in} T_{out} \rho_s(\lambda) t_{paint}^2(\lambda)}{1 - r_d \rho_s(\lambda) t_{paint}^2(\lambda)} \tag{16}$$

This is the Clapper–Yule equation for a continuous coating layer. The parameters T_{in}, T_{out}, r_d, and r_s are defined in the same way as previously for the Saunderson correction of the Kubelka–Munk model, and derived from the Fresnel formulae.

The intrinsic transmittance t_{paint} of the paint layer can be deduced from the measured reflectance of the sample, according to the following formula derived from Eq. (16):

$$t_{paint}(\lambda) = \sqrt{\frac{1}{\rho_s(\lambda)} \cdot \frac{R_i(\lambda) - r_s}{T_{in} T_{out} + r_d [R_i(\lambda) - r_s]}} \tag{17}$$

2.5. Application to the Codex Borbonicus: assumptions and simplifications

Kubelka–Munk model. In our case, every colored layer is a mixture composed of at least two components: the paper substrate of the Codex Borbonicus (coefficients K_s and S_s, and proportion c_s), and the paint, which can be itself a mixture of different pigments (coefficients K_i and S_i and proportions c_i, $i = 1, 2, \dots$). By assuming that the substrate is totally impregnated of paint and that the scattering coefficient of the substrate is much larger than the ones of the pigments, Duncan's law can be written [26] as:

$$\left(\frac{K}{S}\right)_{mix} = \frac{c_s K_s + c_1 K_1 + c_2 K_2 + \cdots}{c_s S_s} = \frac{K_s}{S_s} + \frac{c_1 K_1 + c_2 K_2 + \cdots}{(1 - c_1 - c_2 - \cdots) S_s} \tag{18}$$

If the respective proportions of the components in the mixture are known, only two measurements are needed to derive the remission function of the paint itself, independently of the substrate: a reflectance measurement on the unpainted substrate and a reflectance measurement on the painted substrate.

For example, when the paint mixed with the substrate contains one colorant (coefficients K_1 and S_1), for example, a red or a yellow pigment, with a proportion $c_1 = 1 - c_s$, the remission function is:

$$\left(\frac{K}{S}\right)_{mix} = \frac{K_s}{S_s} + \frac{c_1}{1 - c_1} \cdot \frac{K_1}{S_s} \tag{19}$$

and when the paint is a mixture of two different pigments labeled 1 and 2, with respective proportions c_1 and c_2 before application on the substrate, the remission function of the mixture is:

$$\left(\frac{K}{S}\right)_{mix} = \frac{K_s}{S_s} + \frac{c'_1}{(1 - c'_1 - c'_2)} \cdot \frac{K_1}{S_s} + \frac{c'_2}{(1 - c'_1 - c'_2)} \times \frac{K_2}{S_s} \tag{20}$$

where c'_1 and c'_2 denote the proportions of the pigments in the mixture of paint and substrate.

Saunderson correction for the Kubelka–Munk model. Our measurements have been done under the diffuse 45° geometry: the Codex Borbonicus is illuminated by a diffuse light and is observed at the observation angle $\theta = 45°$. Assuming that the optical index for paints and paper is $n = 1.5$, it is possible to numerically express the parameters of the Saunderson correction from Eq. (15). By computing Eqs. (11) to (14), we obtain the following values: $r_s = 0.05$, $r_d = 0.6$, $T_{in} = 0.9$,

and $T_{out} = 0.42$ for respectively the specularly reflected light, diffuse light, downward and upward transmitted light at the interface air/paint.

Clapper–Yule model. As for the Kubelka–Munk model, every colored layer is assumed to be composed of at least two components. The difference is that instead of being a mixture, it is a superimposition of the paper substrate of the Codex Borbonicus, and a painted layer which can be itself the superimposition of two different paints (intrinsic transmittances t_i, $i = 1, 2, \dots$).

In our case, the thickness of a layer of paint is unknown and can easily vary from one layer to another and cause variations on the surface. According to the Beer–Lambert law, the thickness of a colorant can be taken into account by rising its transmittance to a power x, proportional to the layer thickness.

For example, when the observed color is composed of one layer of paint on top of the substrate with a transmittance t_1, the reflectance of this superimposition can be written as:

$$R_{sup}(\lambda) = r_s + \frac{T_{in} T_{out} \rho_s(\lambda) t_1^{2x}(\lambda)}{1 - r_d \rho_s(\lambda) t_1^{2x}(\lambda)}$$

and when it is composed of two superimposed colorants on top of the substrate, the reflectance can be written as:

$$R_{sup}(\lambda) = r_s + \frac{T_{in} T_{out} \rho_s(\lambda) t_1^{2x}(\lambda) t_2^{2y}(\lambda)}{1 - r_d \rho_s(\lambda) t_1^{2x}(\lambda) t_2^{2y}(\lambda)}$$

where x is proportional to the thickness of the colored layer 1 and y to the thickness of the colored layer 2.

Determination of the unknowns. In each of these theoretical models, a few parameters are unknown and must be fitted by optimization in order to obtain the best agreement between the simulated and measured spectral reflectances. The simulations are hence carried out by minimizing the difference between the modeled spectrum and the experimental spectrum. This is done through the calculation of the root-mean-square deviation (RMSD) between the two datasets on the whole spectra. The minimization of this mathematical difference generates solutions for the unknown parameters. One should remark here that there is one set of equations for each sample of the spectra (at each wavelength), which means that the calculated optimal values are a compromise that takes into account the entire spectra. The careful study of these resulting optimal values and the comparison of the simulated/experimental spectra in turn helps evaluating the realism of the simulation.

3. Results and discussion

Orange mixture(s). The hypothesis for the orange color is that it is made of a mixture of red and yellow materials impregnated into the paper substrate of the document. The Kubelka–Munk model is the most appropriate in this case. It is applied on the intrinsic spectral reflectance of the colored material, after having removed the optical effects of the material/air interface thanks to the inversed Saunderson correction applied on the measured spectral reflectance of the sample, according to Eq. (15).

The calculation involves four diffuse reflection experimental measurements (substrate, red, yellow, and orange). The remission function of the substrate is firstly calculated according to Eq. (7). The reflection spectra measured in each primary color (red and yellow) can then be integrated into Eq. (19), and the remission function of the two colors impregnated in the paper substrate is deduced:

$$\frac{K_{Red}}{S_{Substrate}} = \frac{(1 - C_{Red})}{(C_{Red})} \cdot \left(\left(\frac{K}{S} \right)_{Red\ (measured)} - \left(\frac{K}{S} \right)_{Substrate\ (measured)} \right) \tag{21}$$

$$\frac{K_{Yellow}}{S_{Substrate}} = \frac{(1 - C_{Yellow})}{(C_{Yellow})} \cdot \left(\left(\frac{K}{S} \right)_{Yellow\ (measured)} - \left(\frac{K}{S} \right)_{Substrate\ (measured)} \right) \tag{22}$$

Notice that the two concentration factors that represent the color/substrate proportions C_{Red} and C_{Yellow} are unknown and non-measurable.

The remission function of the red and yellow mixture is then expressed as (see Eq. (20)):

$$\left(\frac{K}{S} \right)_{Mixture} = \left(\frac{K}{S} \right)_{Substrate} + \frac{C'_{Red}}{(1 - (C'_{Red} + C'_{Yellow})} \frac{K_{Red}}{S_{Substrate}} + \frac{C'_{Yellow}}{(1 - (C'_{Red} + C'_{Yellow})} \frac{K_{Yellow}}{S_{Substrate}} \tag{23}$$

Again, two other proportion factors in the mixture C'_{Red} and C'_{Yellow} are necessary and unknown.

As a result, a system in four unknowns is obtained, and its resolution is impossible without any other information. The simulations can still be carried out by determining the optimal proportion values in order to minimize the difference between the measured and predicted spectral reflectances of the mixture. The results of this simulation are given in Fig. 5.

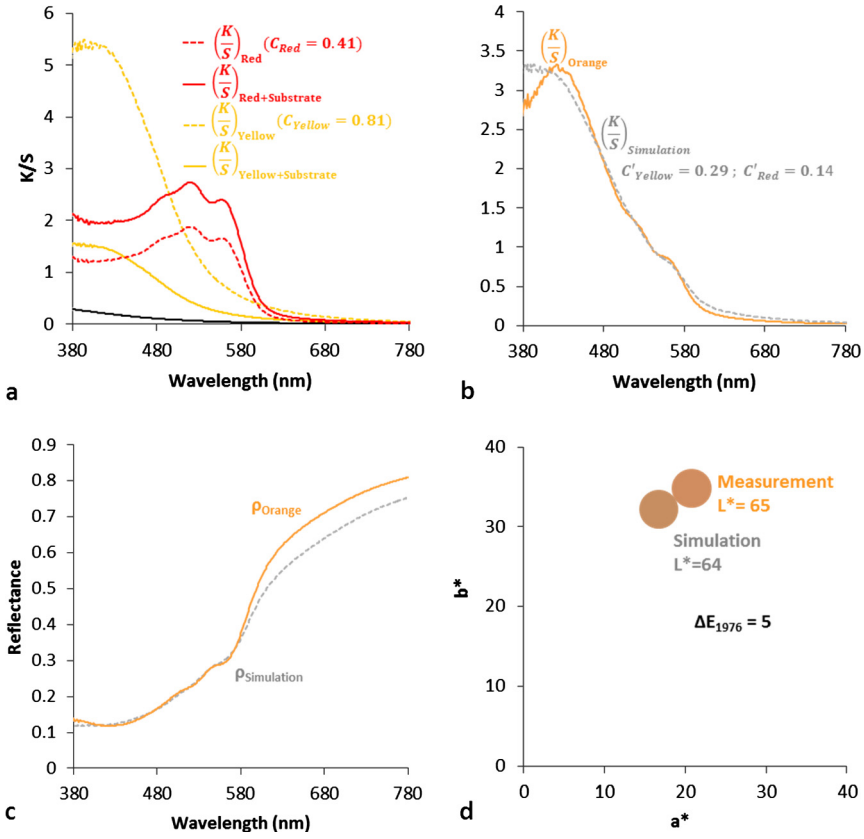

Fig. 5. (**a**) Remission functions deduced from the spectral reflectance measurements for the uncovered substrate, and the red areas and yellow areas (solid lines), and simulated remission functions for the red and yellow areas independently from the absorbance of the substrate (dashed lines). (**b**) Remission function for the orange deduced from the reflectance measurement (solid line), and simulated from the remission functions of the red and the yellow (dashed grey line). (**c**) Corresponding measured and simulated spectral reflectances. (**d**) CIE 1976 $L^*a^*b^*$ colorimetric coordinates projected on the (a^*–b^*) plane with color disks indicating the RGB rendering.

The concentration factors calculated in the first part of the simulation seem coherent, since they are of similar order of magnitude for the two primary colors deposited on the paper substrate ($C_{\text{Red}} = 0.41$, $C_{\text{Yellow}} = 0.81$). The combination of the three remission functions associated with the red, yellow, and substrate generates a simulated remission function for the orange color relatively close to the one deduced from the experimental measurement (Fig. 5b). The concentration factors are slightly lower ($C'_{\text{Red}} = 0.14$; $C'_{\text{Yellow}} = 0.29$) than when the colors are used alone. These coefficients are realistic, and it is not surprising that smaller amounts are used in the mixture. The local absorbance maxima positioned at 525 and 560 nm are present in the simulation at the right intensity, while the absorption edge is also properly positioned. A non-negligible difference between simulation and measurement is however observed with an under-estimation of the calculated remission function for high absorptions, i.e. between 380 nm and 480 nm.

Considering the spectral reflectance calculated from this simulated remission function of the orange paint, a better matching is found in the problematic range (Fig. 5c). This observation is logical since data representation in reflectance is less sensitive to strong absorption values. The comparison of the corresponding simulated and experimental colorimetric data gives a color difference at the limit of human perception ($\Delta E_{1976} = 5$) (Fig. 5d).

Different orange tonalities actually also exist in the document (not shown). These chromatic variations probably originate from different proportions of substrate and red and yellow materials. The reliability of the simulation to explain these variations must be evaluated. For that purpose, the previously calculated remission functions (K/S_{Red} and K/S_{Yellow}) for the primary colors are used (Fig. 5a, dotted lines). The concentration factors of the two primary colors obtained in the first mixture simulation (C_{Red} and C_{Yellow}) are now fixed (0.41 and 0.81, respectively) and not modified afterward for the other orange shades. The calculation still involves an optimization of the concentration factors (C'_{Red} and C'_{Yellow}) in the orange mixtures that minimizes the difference with the experimental data.

Two spectral reflectances measured in areas of the Codex Borbonicus presenting different shades of orange hence generated two couples of concentration factors. Although the calculation exclusively involved the remission functions, only the experimental and simulated reflection spectra are presented (Fig. 6a and b). In each case, the simulation generates a spectral profile close to the experimental data. The associated colorimetric differences are below the limit of human perception ($\Delta E_{1976} < 5$).

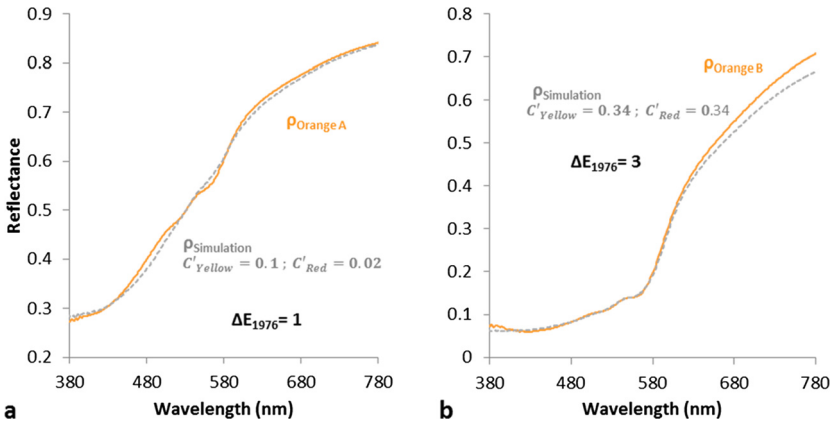

Fig. 6. Spectral reflectances of two orange areas (continuous orange lines) and simulated spectral reflectance corresponding to different mixtures of red and yellow materials (dashed grey lines).

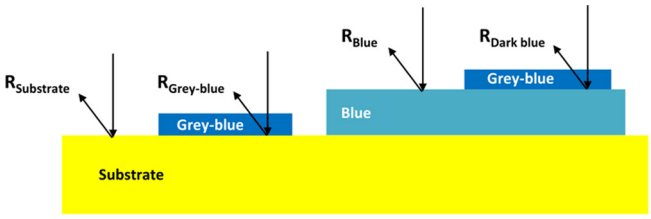

Fig. 7. Hypothetical structure of the dark-blue paint of the Codex Borbonicus.

However, a closer look at the simulation of the lightest orange shade (OrangeA, presenting the highest reflectance levels) is important. The local absorbance maxima at 525 and 560 nm are not present in the calculated mixture (Fig. 6a), although the colorimetric correspondence is very good. This is explained by the very low calculated concentration factors of the red component that result in a weak representation of its spectral features. In contrast, the features are well simulated for the darker variation (OrangeB), although the colorimetric difference is slightly higher, probably due to an offset in the calculated and actual reflection levels at the longer wavelengths of the domain. Notice that, in this case, the red and yellow concentration factors are of the same order of magnitude.

These data show that the simulation can take into account the variations of the concentrations of the primary materials as long as they are present in amounts of the same order of magnitude when they are used alone and mixed (OrangeB). When much lower amounts are involved in the simulation (OrangeA), poorer spectral correspondences are calculated (although the color shift is almost null). Caution must be taken when evaluating a spectral correspondence. A small color difference ($\Delta E_{1976} < 5$) does not necessarily imply a satisfying simulation from a spectral standpoint. It is therefore important to focus on the presence, position, and intensity of material specific spectral features.

In any case, and more importantly, these results demonstrate that it is indeed possible to successfully simulate the mixture of the red and yellow primary colors to obtain the experimental spectrum measured in the different orange hues of the Codex Borbonicus. They hence reinforce the hypothesis that the orange paint was obtained by a mixture of the yellow and red paints (and not with the use of other coloring materials).

Dark blue. The visual examination of the dark-blue paint of the Codex Borbonicus suggests that it has been obtained by superimposition of a layer of grey-blue material on top of layer of blue material.

Assuming that the grey-blue paint does not scatter light, that the blue paint is opaque and homogeneous, and that there are no reflections at the grey-blue/blue and grey-blue/substrate interface, a first simplistic attempt at simulating this color association is done by evaluating the transmission profile of the grey-blue paint with the measurement of its reflection properties – Fig. 7 and Eq. (24). The result of the superimposition of the grey blue on the blue is then found by applying this calculated transmission to the reflection spectrum measured in the blue – Fig. 7 and Eq. (25). The layer thickness of the grey blue on the substrate and on the blue being probably different, the x factor is used to fit this variation and is unknown.

$$T_{\text{Grey blue}} = \sqrt{\frac{R_{\text{Grey blue}}}{R_{\text{Substrate}}}} \tag{24}$$

$$R_{\text{Grey blue on blue (calculated)}} = R_{\text{Blue}} T^{x}_{\text{Grey blue}} = (R_{\text{Dark blue (measured)}}?) \tag{25}$$

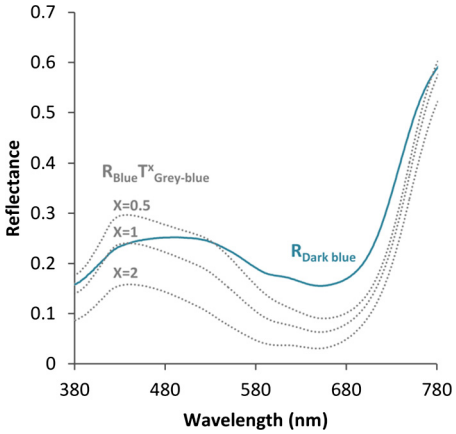

Fig. 8. Diffuse reflection spectrum of the dark-blue paint (blue continuous line) and simplistic simulation of the superimposition of grey-blue on top of blue with different thicknesses (x) of the grey-blue layer (grey dotted lines).

When fitting the thickness of the grey-blue layer to $x = 2$, a spectral shape close to the experimental spectrum is obtained, but the global reflection level is too low (Fig. 8). In contrast, a low thickness index ($x = 0.5$) generates a closer general level of reflection, but the spectral feature of the experimental spectrum (absorption maximum at 590 nm) is absent from the simulation. This preliminary simulation does not provide satisfying results: we thus explored a different approach, by taking into account the air/paint interface.

The Clapper–Yule model is used since it can take into account a partial impregnation of the grey-blue in the underlying layers (substrate or blue). This model involves the transmittances of both the blue paint and the grey-blue paint. According to the Eq. (17), these are given by the following expressions:

$$t_{\text{Blue}}(\lambda) = \sqrt{\frac{1}{\rho_s(\lambda)} \cdot \frac{R_{\text{Blue}}(\lambda) - r_s}{T_{\text{in}} T_{\text{out}} + r_d [R_{\text{Blue}}(\lambda) - r_s]}}$$

$$t_{\text{Grey blue}}(\lambda) = \sqrt{\frac{1}{\rho_s(\lambda)} \cdot \frac{R_{\text{Grey blue}}(\lambda) - r_s}{T_{\text{in}} T_{\text{out}} + r_d [R_{\text{Grey blue}}(\lambda) - r_s]}}$$

where $R_{\text{Blue}}(\lambda)$ and $R_{\text{Grey blue}}(\lambda)$ denote the spectral reflectances of areas painted in blue alone, respectively in grey-blue alone, and $\rho_s(\lambda)$ denotes the intrinsic reflectance of the substrate.

The observation geometry being known ($\theta = 45°$), and the paints optical indices being assumed to be $n = 1.5$ (see above the section on the Saunderson correction), we still have: $r_s = 0.05$, $r_d = 0.6$, $T_{\text{in}} = 0.9$ and $T_{\text{out}} = 0.42$.

Consequently, we derive the theoretical reflectance of the dark blue. Let us consider the parameters X and Y that are proportional to the thickness of the blue and grey blue painted layers.

$$R_{\text{Dark blue}}(\lambda) = r_s + \frac{T_{\text{in}}\, T_{\text{out}}\, \rho_s(\lambda)\, t^X_{\text{Grey blue}}(\lambda)\, t^Y_{\text{Blue}}(\lambda)}{1 - r_d\, \rho_s(\lambda)\, t^X_{\text{Grey blue}}(\lambda)\, t^Y_{\text{Dark blue}}(\lambda)}$$

Because of the two unknown parameters X and Y, our system is not solvable. As for the Kubelka–Munk model, the simulation is made finding optimal thickness values.

The results of our optimization are not physical thicknesses: X and Y are only proportional to the actual thicknesses of the layers. As the light is going onto and out of the paints, we can then assume that they are proportional to at least two times the real thickness of each painted layer. Nevertheless, these two parameters are both in the same range ($X = 0.87$ and $Y = 1.19$) and so can be considered as reliable results (Fig. 9).

Although the spectral correspondence is not perfect, all the absorption features present in the experimental spectrum are found in the calculated superimposition at the right reflectance level. The colorimetric difference between the simulated and hypothetical experimental superimposition is also satisfying. The success of this simulation strengthens the hypothesis that the dark blue was obtained through a superimposition of grey blue on top of blue.

4. Conclusion

The present paper illustrates the use of optical models to make a first assessment on the composition and structure of colored components in historical polychromies from non-invasive spectral reflectance measurements. The layered structure of the polychromies is generally unknown, but it has an impact on the way the light is reflected, therefore on the way the light signal must be analyzed in order to determine the material combination. We introduced two models, based on two

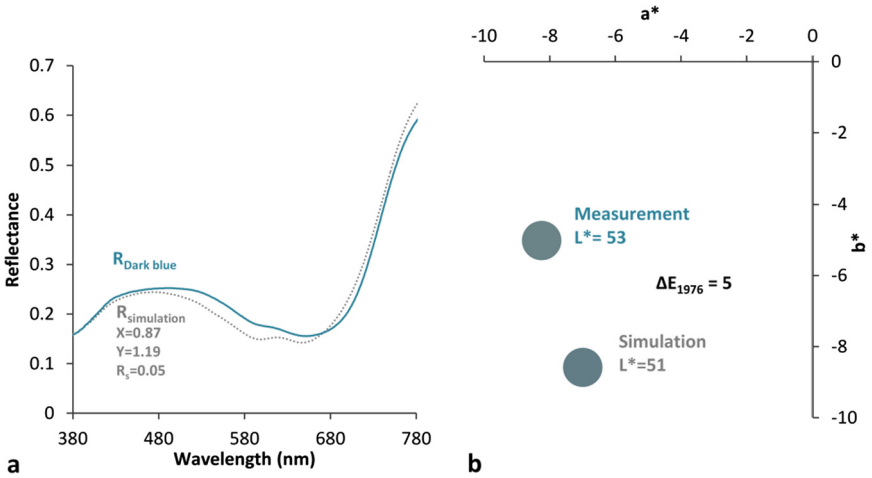

Fig. 9. (a) Spectral reflectance of the dark-blue paint, as measured (blue solid line) and simulated by the Clapper–Yule model for a superimposition of grey-blue and blue layers with a partial impregnation of the grey blue in the underlying substrate (grey dotted lines). **(b)** Corresponding CIE 1976 $L^*a^*b^*$ colorimetric coordinates projected onto the (a^*–b^*) plane and disk showing the RGB rendering.

different layered structures, whose advantage is to be compatible with diffuse spectroscopy: the intrinsic optical parameters of the materials are derived from the experimental reflectance spectra. The Kubelka–Munk model, with Saunderson correction to take into account the optical effect of the air/paint interface, applies to opaque paints where it can be assumed that the light is mainly reflected by a uniform, macroscopically homogenous, and diffusing colored layer (e.g., substrate impregnated of paint). The Clapper–Yule model, used for continuous colored layers, applies to a non-scattering layer, or weakly scattering layer, on top of a colored diffusing background. It also takes into account the optical effect of the air/paint interface. When the materials (e.g., pigments, substrate, ...) mixed in the paint are known, simulations can be performed by varying the proportions of the different materials, and by searching the proportions giving the best agreement with the spectral reflectance measured on the object. This helps to evaluate the plausibility of hypotheses made on the structure of complex colored mixtures.

An important issue concerns the way the parameters are computed, i.e. the optimization process used to find the best agreement between the simulated and measured spectral reflectances. When applying the models to experimental data, several parameters are unknown. As a result, the simulations are carried out as comparison with the experimental measurement on the paint layer for which the hypothesis is made. The minimization of the distance between the modeled and experimental spectra is used to optimize the unknowns of the system. The spectral distance selected as cost function in the optimization can have a significant influence on the results. In this study, we used the RMSD distance. The colorimetric difference (ΔE) can also be of interest to compare the spectra, although one must be aware that a good color match does not necessarily imply a satisfying spectral correspondence (see the results of the orange mixture simulation). Other types of spectral distances exist (such as the spectral angle, for example [27]) and should be considered for future research [28]. An experimental study of color combinations of known composition will help to evaluate the appropriate spectral distances and the application ranges of the presented optical models.

Acknowledgements

The authors wish to thank Mr. Patrick Montambault and Mrs. Éliane Fighiera for granting access and allowing the measurements on the *Codex Borbonicus*. They also thank the "Assemblée nationale" and the "Fondation des sciences du patrimoine/Labex Patrima" (ANR-10-LABX-0094-01) for having funded this study.

References

[1] H. Kunkely, A. Vogler, Absorption and luminescence spectra of cochineal, Inorg. Chem. Commun. 14 (2011) 1153–1155, https://doi.org/10.1016/j.inoche.2011.04.011.
[2] C. Zaffino, A. Passaretti, G. Poldi, M. Fratelli, A. Tibiletti, R. Bestetti, I. Saccani, V. Guglielmi, S. Bruni, A multi-technique approach to the chemical characterization of colored inks in contemporary art: the materials of Lucio Fontana, J. Cult. Herit. (2016), https://doi.org/10.1016/j.culher.2016.09.006.
[3] A. Casini, C. Cucci, M. Picollo, L. Stefani, T. Vitorino, Creation of a hyper-spectral imaging reference database, COSCH e-Bull. 2 (2015) 1–6.
[4] T. Vitorino, A. Casini, C. Cucci, M.J. Melo, M. Picollo, L. Stefani, Hyper-spectral acquisition on historically accurate reconstructions of red organic lakes, in: A. Elmoataz, O. Lezoray, F. Nouboud, D. Mammass (Eds.), Proc. Image Signal Process 6th Int. Conf. ICISP 2014, Cherbourg, France, 30 June–2 July 2014, Springer International Publishing, 2014, pp. 257–264.
[5] K.M. Morales, B.H. Berrie, A note on characterization of the cochineal dyestuff on wool using microspectrophotometry, E-Preserv. Sci. 12 (2015) 8–14.
[6] C. Montagner, M. Bacci, S. Bracci, R. Freeman, M. Picollo, Library of UV–Vis–NIR reflectance spectra of modern organic dyes from historic pattern-card coloured papers, Spectrochim. Acta, Part A, Mol. Biomol. Spectrosc. 79 (2011) 1669–1680, https://doi.org/10.1016/j.saa.2011.05.033.

[7] M.A. Maynez-Rojas, E. Casanova-González, J.L. Ruvalcaba-Sil, Identification of natural red and purple dyes on textiles by Fiber-optics Reflectance Spectroscopy, Spectrochim. Acta, Part A, Mol. Biomol. Spectrosc. 178 (2017) 239–250, https://doi.org/10.1016/j.saa.2017.02.019.
[8] M. Hébert, R.D. Hersch, Review of spectral reflectance models for halftone prints: principles, calibration, and prediction accuracy, Color Res. Appl. 40 (2015) 383–397, https://doi.org/10.1002/col.21907.Review.
[9] D. Duncan, The colour of pigment mixtures, J. Oil Colour Chem. Assoc. 32 (1949) 296–321.
[10] A.R. Pallipurath, J.M. Skelton, P. Ricciardi, S.R. Elliott, Estimation of semiconductor-like pigment concentrations in paint mixtures and their differentiation from paint layers using first-derivative reflectance spectra, Talanta 154 (2016) 63–72, https://doi.org/10.1016/j.talanta.2016.03.052.
[11] J.M. Fernández Rodríguez, J.A. Fernández Fernández, Application of the second derivative of the Kubelka–Munk function to the semiquantitative analysis of Roman paintings, Color Res. Appl. 30 (2005) 448–456, https://doi.org/10.1002/col.20157.
[12] G. Dupuis, M. Menu, Quantitative characterisation of pigment mixtures used in art by fibre-optics diffuse-reflectance spectroscopy, Appl. Phys. A, Mater. Sci. Process. 83 (2006) 469–474, https://doi.org/10.1007/s00339-006-3522-3.
[13] F. Pottier, A. Michelin, C. Andraud, F. Goubard, B. Lavédrine, Characterizing the intrinsic fluorescence properties of historical painting materials: the case study of a sixteenth-century Mesoamerican manuscript, Appl. Spectrosc. 72 (2018) 573–583, https://doi.org/10.1177/0003702817747276.
[14] F. Pottier, Etude des matières picturales du Codex Borbonicus – Apport des spectroscopies non-invasives à la codicologie, Université de Cergy-Pontoise, France, 2017.
[15] F. Pottier, S. Kwimang, A. Michelin, C. Andraud, F. Goubard, B. Lavédrine, Independent macroscopic chemical mappings of cultural heritage materials with reflectance imaging spectroscopy: case study of a 16th century Aztec manuscript, Anal. Methods 9 (2017) 5997–6008, https://doi.org/10.1039/C7AY00749C.
[16] F. Pottier, A. Michelin, G.B. Anne, A. Tournié, F. Goubard, A. Histace, B. Lavédrine, Preliminary investigation on the Codex Borbonicus: macroscopic examination and coloring materials characterization, in: E. Dupey-Garcia, M. Vazquez de Agredos (Eds.), Colors on the Skin, The University of Arizona Press, Tucson, AZ, USA, 2018, in press.
[17] P. Kubelka, F. Munk, Ein Beitrag zur Optik des Farbanstriche, Z. Tech. Phys. 12 (1931) 593–601.
[18] M. Hébert, R.D. Hersch, Extending the Clapper–Yule model to rough printing supports, J. Opt. Soc. Am. A, Opt. Image Sci. Vis. 22 (2005) 1952–1967, https://doi.org/10.1364/JOSAA.22.001952.
[19] J.L. Saunderson, Calculation of the color pigmented plastics, J. Opt. Soc. Am. 32 (1942) 727–736.
[20] D.B. Judd, Fresnel reflection of diffusely incident light, J. Res. Natl. Bur. Stand. 29 (1942) 329–332 (1934).
[21] S.Q. Duntley, The optical properties of diffusing materials, J. Opt. Soc. Am. 3 (1942) 61–70.
[22] F.C. Williams, F.R. Clapper, Multiple internal reflections in photographic color prints, J. Opt. Soc. Am. 43 (1953) 595–597.
[23] J.D. Shore, J.P. Spoonhower, Reflection density in photographic color prints: generalizations of the Williams–Clapper transform, J. Imaging Sci. Technol. 45 (2001) 484–488.
[24] F.R. Clapper, A.C. Yule, The effect of multiple internal reflections on the densities of halftone prints on paper, J. Opt. Soc. Am. 43 (1953) 600–603.
[25] M. Hebert, R.D. Hersch, Deducing ink-transmittance spectra from reflectance and transmittance measurements of prints, Proc. Soc. Photo-Opt. Instrum. Eng. 649314 (2007), https://doi.org/10.1117/12.705951.
[26] R.S. Berns, M. Mohammadi, Evaluating single- and two-constant Kubelka–Munk turbid media theory for instrumental-based inpainting, Stud. Conserv. 52 (2007) 299–314.
[27] R.H. Yuhas, A.F.H. Goetz, J.W. Boardman, Discrimination among semiarid landscape endmembers using the spectral angle mapper (SAM) algorithm, in: R.O. Green (Ed.), Summaries of the Third JPL Airborne Geoscience Workshop, vol. 1, JPL Publication, 1992, pp. 147–149.
[28] H. Deborah, N. Richard, J.Y. Hardeberg, A comprehensive evaluation of spectral distance functions and metrics for hyperspectral image processing, IEEE J. Sel. Top. Appl. Earth Obs. Remote Sens. 8 (2015) 3224–3234, https://doi.org/10.1109/JSTARS.2015.2403257.